MINOR FAULT DETECTION BY INTEGRATION OF SEISMIC ATTRIBUTES IN AN OIL RESERVOIR

M.R. BAKHTIARI[1], M.A. RIAHI[2] and K. TINGDAHL[3]

[1] *Faculty of petroleum engineering, University of Amirkabir, P.O. Box 15875-4413, Tehran, Iran. RBakhtiari@aut.ac.ir*
[2] *Institute of Geophysics, University of Tehran, P.O. Box 14155-6466, Tehran, Iran.*
[3] *dGB Earth Sciences, One Sugar Creek Center Blvd., Suite 935, Sugar Land, TX 77478, U.S.A.*

(Received January 23, 2008; revised version accepted April 3, 2009)

ABSTRACT

Bakhtiari, M.R., Riahi, M.A. and Tingdahl, K., 2009. Minor fault detection by integration of seismic attributes in an oil reservoir. *Journal of Seismic Exploration*, 18: 289-304.

Seismic section can often help detect the exact location and movement of minor faults, but sometimes the poor quality of the data makes that impossible. It is well known that the existence of minor faults and fractures in an oil reservoir play an important role in increasing its productivity. The minor faults may cut the cap rock and cause the oil to leak from the reservoir. So, before making any decisions for drilling in an oil field it is very important to know the exact locations of minor faults. In order to detect minor faults, a single seismic attribute is usually applied, but the results are not satisfactory. In this paper, for minor fault detection, we introduce a method based on a combination of seismic attributes in a Neural Network system. Firstly, different attributes like energy, similarity, dip variance, polar dip and polar dip angle with different time gates were applied on a seismic section. Then to combine these attributes together and apply them, a workflow was constructed, in which an artificial neural network system was designed, the above-mentioned attributes were introduced to the system and hand-picked faults were input to the ANN system. When the training of the system completes, the ANN estimates an output cube that indicates the faults location. The obtained results based on this study showed that using a combination of attributes in the ANN system is more reliable than applying a single attribute to locate the minor faults in an oil reservoir.

KEYWORDS: minor fault, oil reservoir, seismic attributes, neural network system, output cube.

0963-0651/09/$5.00

INTRODUCTION

In a conventional seismic interpretation project, usually for fault picking purposes, a direct fault picking method is applied. In this method the interpreter will look for the fault on the seismic section based on similarity among the layers. Faults are therefore located either by hand, i.e. by drawing a few lines on the final plot of a seismic line, or by using interpretation software. Some of the recent interpretation methods have provided seismic attribute calculation for fault detection. Such methods are incapable of tracing subtle faults. In fault detection, based on attribute study, coherency or variance cube attributes are usually applied. This type of study provides very good results while the data are of good quality. If the data are not of good quality or a major fault is not present on the seismic section, the application of single attribute will not be adequate.

In order to overcome the above shortcomings in fault detection, we have attempted to use an Artificial Neural Network (ANN) system as transfer function. In this approach, the interpreter indicates some places on the seismic section that have a high probability of being faults, he will then input these data to the ANN system. When training of the system completes, the ANN estimates an output cube that highlights the fault locations. In a single attribute study, the applied attribute must be powerful, but in the ANN approach there is no limitation in application of certain attributes for fault detection. In the ANN method, the only condition that has to be taken into account is that different weights should be considered for different attributes in fault location detection.

To achieve a good result, we have designed a proper ANN system by examining different types of attributes with different weights that has led to an output cube in-which we can indicate the faults.

GEOLOGY OF THE STUDY AREA

This study is focused on the Ab-Teymur anticline. The Ab-Teymur structure is a gentle NW-SE trending anticline formed in response to a NE compression during the Zagros orogeny. The neighboring Mansuri and Susangerd anticlines are located in SE and NW of the Ab-Teymur field respectively with a small lateral offset. These anticlines are the three outermost structures of the Zagros folded belt located far from the Zagros suture zone.

There is a transition from the Zagros trends to the Arabian N-S structures. The Ab-Teymur anticline is located on the northeastern edge of this transition zone. The eastward extent of the Arabian plate structures prior to the Zagros folding is uncertain; however it is likely that an N-S grain underlies structures

such as Ab-Teymur and Mansuri. This may have controlled early structural features, sedimentation and fracture trends.

The results of this study are based on seismic data acquired from the Ab-Teymur anticline located at 15 Km south of Ahwaz in southern Iran. The Ab-Teymur structure is a simple anticline which appears to be unfaulted at the Bangestan and Asmari levels but in the Gachsaran level, it shows some faulted zones.

In this study, we have specifically focused on minor faults in Gachsaran, which is the cap rock of the reservoir. It is therefore very important for us to know how these faults have extended in the cap rock.

The seismic survey was made by NIOC from 1999 until 2001 in an area of 420 km^2. The bin size is 25 by 25 and the foldage 24.

Both source and receiver intervals are 50 meters and the recording length is 7 seconds. The sampling rate of the seismic data is 2 ms and the source of seismic energy is dynamite in the severe topography whilst vibroseis has been used for the gentle topography. Fig. 1 shows the Ab-Teymur anticline location map and its stratigraphy column.

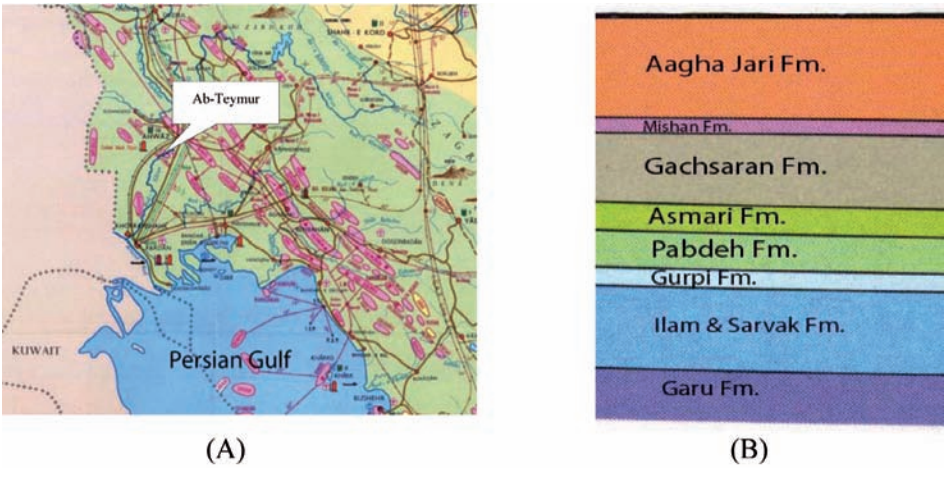

Fig. 1. Ab-Teymur anticline location map (A) and the stratigraphy column (B).

SINGLE ATTRIBUTE STUDY

To verify the ability of a multi attribute study via a single attribute, firstly, we have applied single attribute and then we examined several attributes like energy, similarity, dip variance, polar dip and polar dip angle on a seismic section. Meanwhile, the combination of attributes that we have considered for our ANN system are Curvature, Dip, Energy (with different time gates), Similarity, Spectral Decomposition, Instantaneous Frequency, Instantaneous Phase, Instantaneous Amplitude, Instantaneous Bandwidth and Instantaneous Cosine of Phase.

The cube environment that we have chosen for this study is between inline 1200 - 1300 and cross line 300 - 500 with a time interval between 1200 - 1600 milliseconds. The inline that we have used for our calculations is the line number 1250 and then the ANN system has made calculations on all parts of this cube.

The seismic section that we have used for fault location detection is shown in Fig. 2. The probable locations of faults are manually picked and marked by violet dots and non fault areas are marked by green dots.

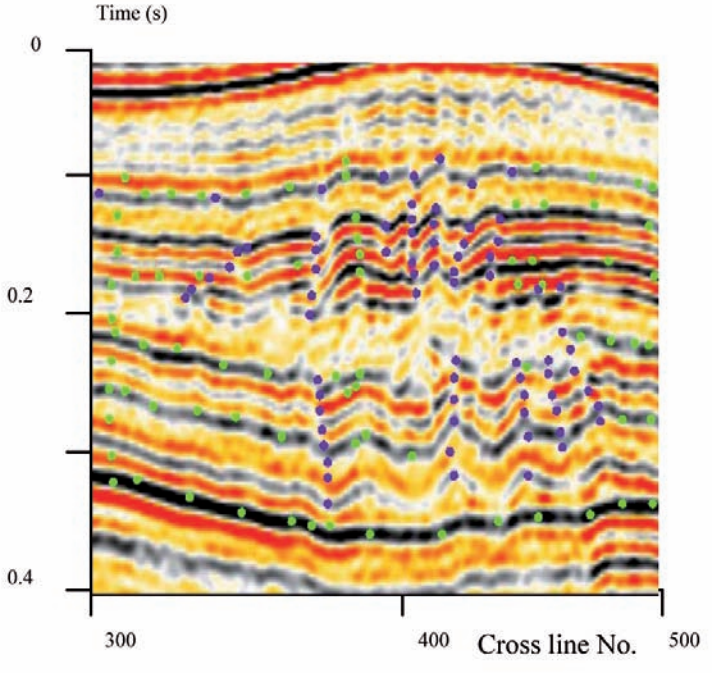

Fig. 2. The seismic section of inline 1250 selected from the cube, between 1200 to 1600 ms TWT. The probable locations of faults are detected based on direct picking method and marked by violet dots. Non fault areas are marked by green dots. The horizontal axis indicates cross-line number.

Energy

Energy is a measure of textural uniformity in an image. Energy is low when all elements in the grey-level co-occurrence matrices (West et al., 2002; Gao, 2003) are equal. It is useful for highlighting geometry and continuity. This attribute calculates the squared sum of the sample values in the specified time gate divided by the number of samples in the same time gate. It reads:

$$E = [\sum_{i=1}^{n} A_i^2]/n \quad . \tag{1}$$

Fig. 3 shows the results obtained after application of the energy attribute on the seismic section shown in Fig. 2, with four different time gates.

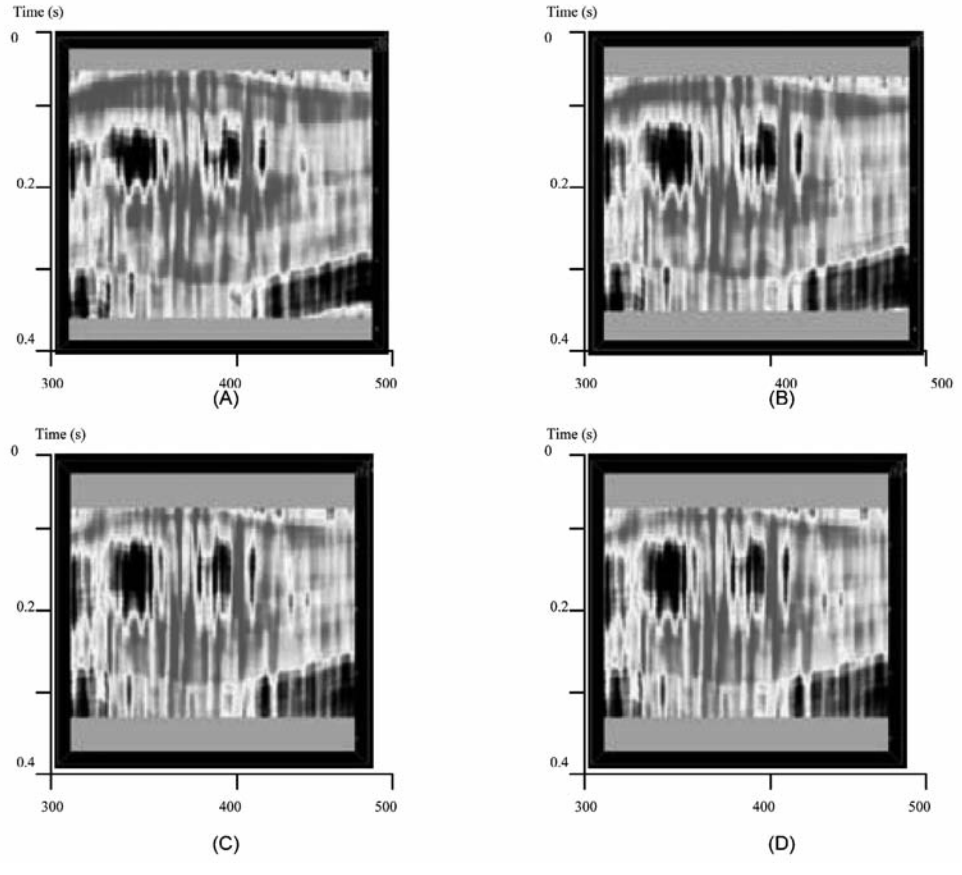

Fig. 3. Energy attribute applied on the same seismic section shown in Fig. 2 with four different time gates: (A) (−32, 32) ms, (B) (−40, 40) ms, (C) (−52, 52) ms, and (D) (−80, 80) ms. Panel D shows the fault locations more clearly than the other panels do.

Similarity

Similarity is a type of "coherency" that expresses how much two or more trace segments look alike. Measuring local similarity between two seismic images is useful for seismic monitoring, registration of multi component data, and analysis of velocities and amplitudes (Fomel, 2007). A similarity of one means the trace segments are identical in waveform and amplitude. A similarity of zero means they are completely non-similar. The similarity attribute is defined by the following equations (Tingdahl and de Rooij, 2005):

$$S = 1 - |v - u|/(|v| + |u|) \quad , \tag{2}$$

where

$$v = \begin{bmatrix} f(t_1, x_v, y_v) \\ f(t_1 + dt, x_v, y_v) \\ \vdots \\ f(t_2 - dt, x_v, y_v) \\ f(t_2, x_v, y_v) \end{bmatrix} \quad , \tag{3}$$

and

$$u = \begin{bmatrix} f(t_1, x_u, y_u) \\ f(t_1 + dt, x_u, y_u) \\ \vdots \\ f(t_2 - dt, x_u, y_u) \\ f(t_2, x_u, y_u) \end{bmatrix} \quad , \tag{4}$$

where d_t is the sampling interval, and t_1, t_2 are the intervals of the time gate, x_v, y_v and x_u, y_u are the two trace positions that have to be compared, and f(t,x,y) is just the amplitude value in a cube (Tingdahl and de Rooij, 2005). Fig. 4 shows a schematic diagram for the calculation of similarity attributes.

Fig. 5 shows the results obtained after application of the similarity attribute on the seismic section shown in Fig. (2), with different time gates. The specifications of the similarity attributes used in Fig. 5 is presented in Table 1.

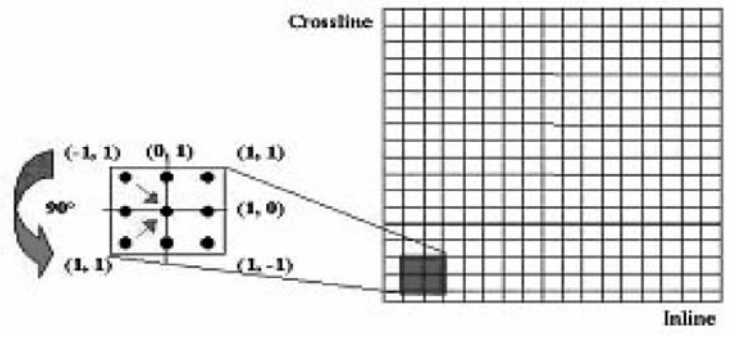

Fig. 4. Schematic diagram for computing similarity attributes of each point using the surrounding points.

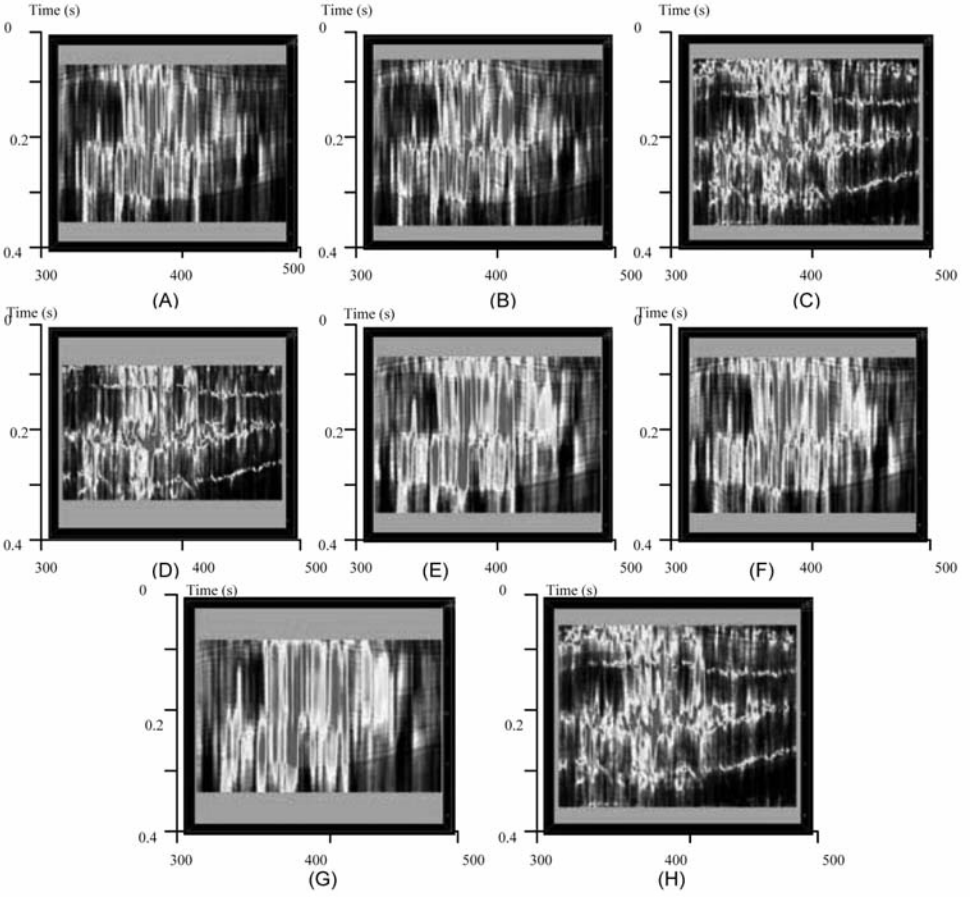

Fig. 5. The results of similarity attribute with different time gates applied on seismic inline 1250.

Table 1. The specifications of the similarity attributes used in Fig. 4. NS = No Steering, FS = Full Steering and min = minimum similarity in output.

Panel	Time Gate	Lateral position	Other settings
A	(−40,40)	(−1,0)(1,0)	NS min
B	(−32,−32)	(−1,0)(1,0)	NS min
C	(−32,32)	(−1,0)(1,0)	FS min
D	(−60,60)	(−1,0)(1,0)	FS min
E	(−40,40)	(−1,2)(1,−2)	NS min
F	(−40,40)	(−1,−1)(1,1)	NS min
G	(−60,60)	(−1,2)(1,−2)	NS min
H	(−32,32)	Step out 1	FS min

Dip Variance

The variance of the dip is calculated in a small sub-volume around the evaluation point. This attribute picks up chaotic reflection patterns. The multi-attribute neural network is based on an object detection method developed by Meldahl et al., (1999). Around the fault location, the dip changes rapidly and for this reason the statistical value of dip changes clearly. Therefore, one of the best attributes that indicates faults is dip variance. This attribute is expressed mathematically by the following formula (Tingdahl and de Rooij, 2005).

$$\mathrm{var}(p_x) = [1/(n-1)] \sum_{\beta=-x_s}^{x_s} \sum_{\alpha=-y_s}^{y_s} \sum_{\tau=-a}^{b} [p_x(x+\alpha,y+\beta,t+\tau) - \bar{p}_x]^2 \quad , \quad (1)$$

where

$$\bar{p}_x = (1/n) \sum_{\beta=-x_s}^{x_s} \sum_{\alpha=-y_s}^{y_s} \sum_{\tau=-a}^{b} [p_x(x+\alpha,y+\beta,t+\tau) \quad , \quad (2)$$

where n is the total number of terms in triple summation, x_s and y_s are the maximum trace stepout and a and b are the relative start and stop time of window or upper and lower limits of the cube and p is the dip value (Tingdahl and de Rooij, 2005). Fig. 6 shows the results obtained after application of the dip variance attribute on inline 1250, shown in Fig. 2, with three different time gates.

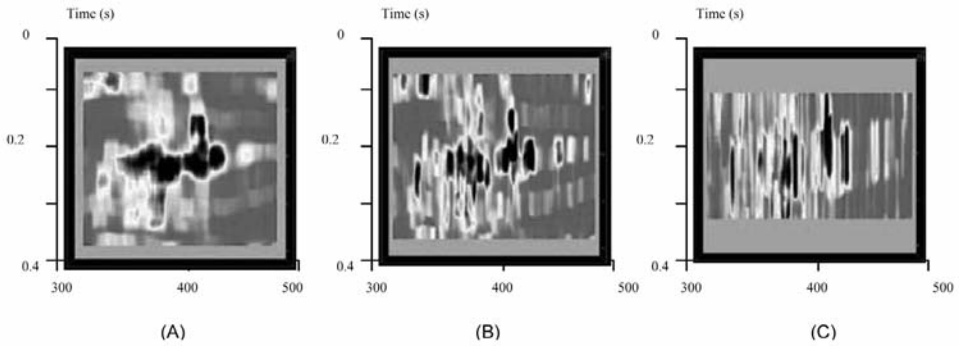

Fig. 6. The results of the dip variance attribute with three different time gates and different settings applied on seismic inline 1250.

Table 2. The specifications of the dip variance attributes used in Fig. 5.

Panel	Time Gate	Lateral Position
A	(−16,16)	Step out 6
B	(−24,24)	Step out 2
C	(−60,60)	Step out 1

Polar dip and Polar dip Angle

Polar dip attribute converts the input orthogonal dips (inline and cross line dip) to true dip (Meldahl et al., 1999). The dip is measured from the horizontal and if the range of the dip is more than zero, this attribute has the maximum value on the faults plane because normally the dip of fault plane is more than the other sides. Polar dip angle returns the true dip from the apparent dip. Fig. 7 shows the results obtained after the application of the polar dip and polar dip angle attributes on inline 1250, shown in Fig. 2.

A comparison between the outputs obtained from the application of the above-mentioned single attributes shows that none of them are convenient for detecting fault location.

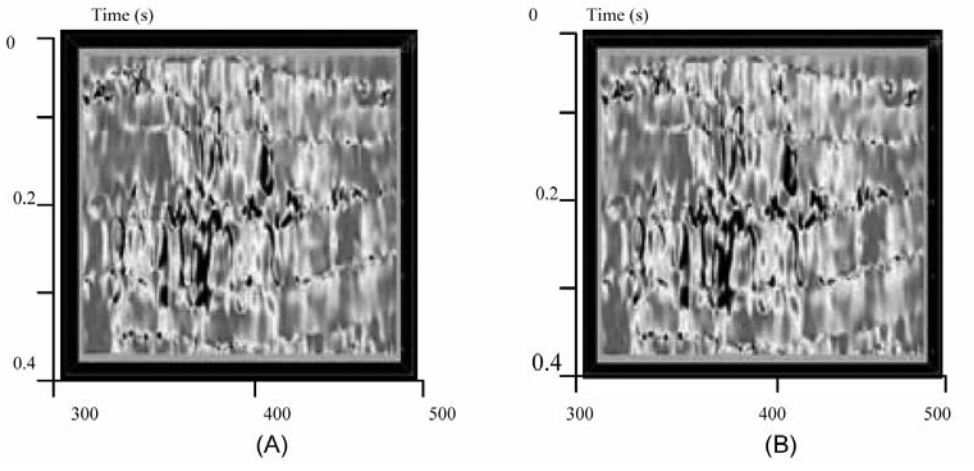

Fig. 7. Polar Dip (A) and Polar dip angle (B) attributes applied on inline 1250. These panels show the extensional faults above the anticline.

It is clear that the above mentioned attributes have their drawbacks as well as their advantages in fault imaging; it means that some attributes are more powerful in fault detection than others but it does not mean that the other attributes not applied here are incapable of fault detection.

In the following section, we introduce a special method based on a combination of different attributes in an integrated approach for fault detection using a neural network system.

THE NEURAL NETWORK RESULTS

The neural network system considers an artificial model like the human brain. The smallest element of a network is like a cell. To make different layers, these cells are connected together. Fig. 8 shows a sketch of a neural network system with an input layer a hidden (middle) layer and an output layer. We usually deal with input and output layers only. To begin with, we used the hand-picked faults on inline 1250 (marked by green dots on Fig. 2) as well as the output of each single attribute on the same line as training input data to the neural network system. Then the neural network scheme was performed. The outputs of the ANN system were two cubes of data, one belonging to the fault cube and the other belonging to the non fault cube. In the ANN approach there is no limitation in the application of certain attributes for fault detection. In the ANN method, the only condition that has to be taken into account is that different weights should be considered for different attributes in fault location

detection. Fig. 9, shows a real neural network window that contains input attributes (right) and matching curve percentage (left), the matching curve percentage was nearly 85% which is a very good matching value.

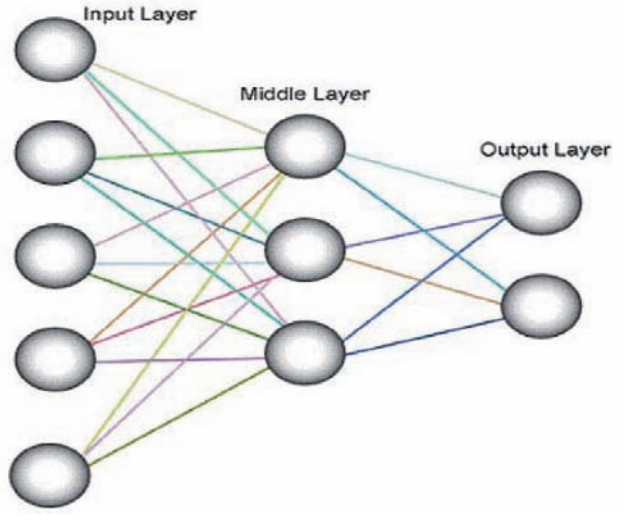

Fig. 8. A multilayer artificial neural network system that contains an input layer (left), a hidden layer (middle) and an output layer (right) (Tingdahl and de Rooij, 2005).

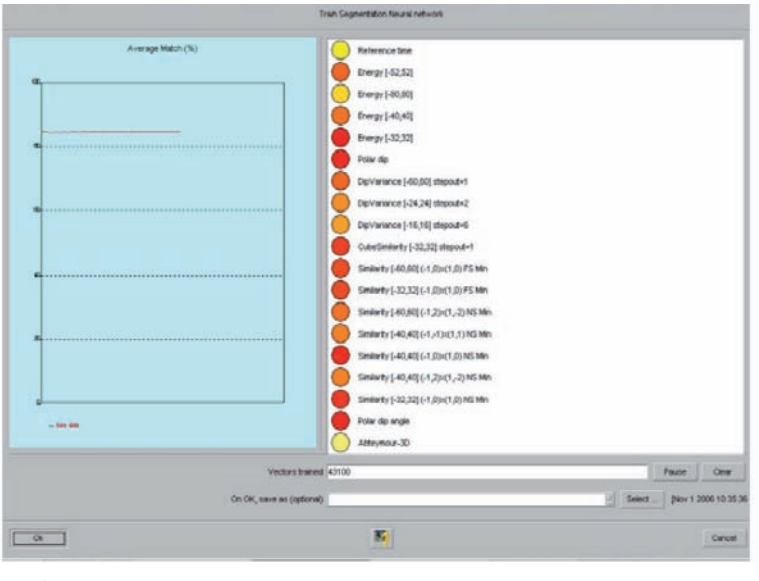

Fig. 9. A real neural network window that contains input attributes (right) and an average match graph (left). The average match is nearly 85%, implying a very good correlation between real seismic data and the output of the neural network system.

Neural network calculations produced two output cubes in the output layer. The first cube is a "Fault Cube" and the second one is a "Non Fault Cube" which are shown in Figs. 10 and 11, respectively. The fault cube and non fault cube show that the inline 1250 cuts through 3 time slices at 100 ms, 200 ms and 300 ms. To investigate the variation of fault orientation, Fig. 12 shows these time slices: a = 100 ms, b = 200 ms and c = 300 ms chosen from the fault cube. The panels A, B and C are close-ups of these time slices.

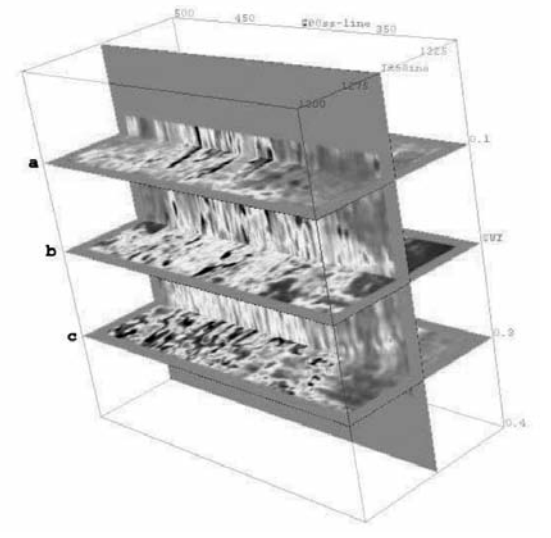

Fig. 10. The fault cube produced by the neural network system. The vertical section is inline 1250 and a, b and c are horizontal time slices at 100 ms, 200 ms and 300 ms, respectively.

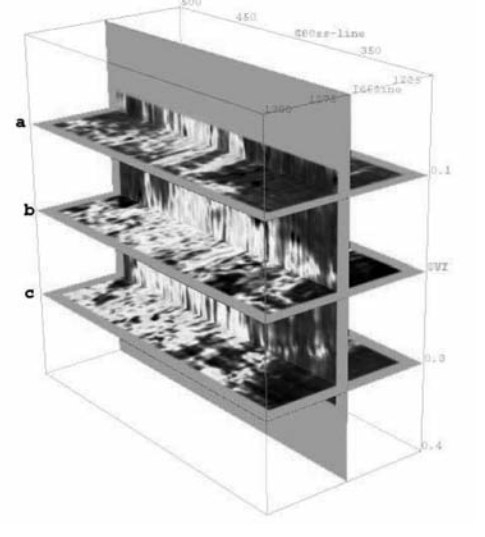

Fig. 11. The non fault cube produced by the neural network system. The vertical section is inline 1250 and a, b and c are time slices at 100 ms, 200 ms and 300 ms, respectively.

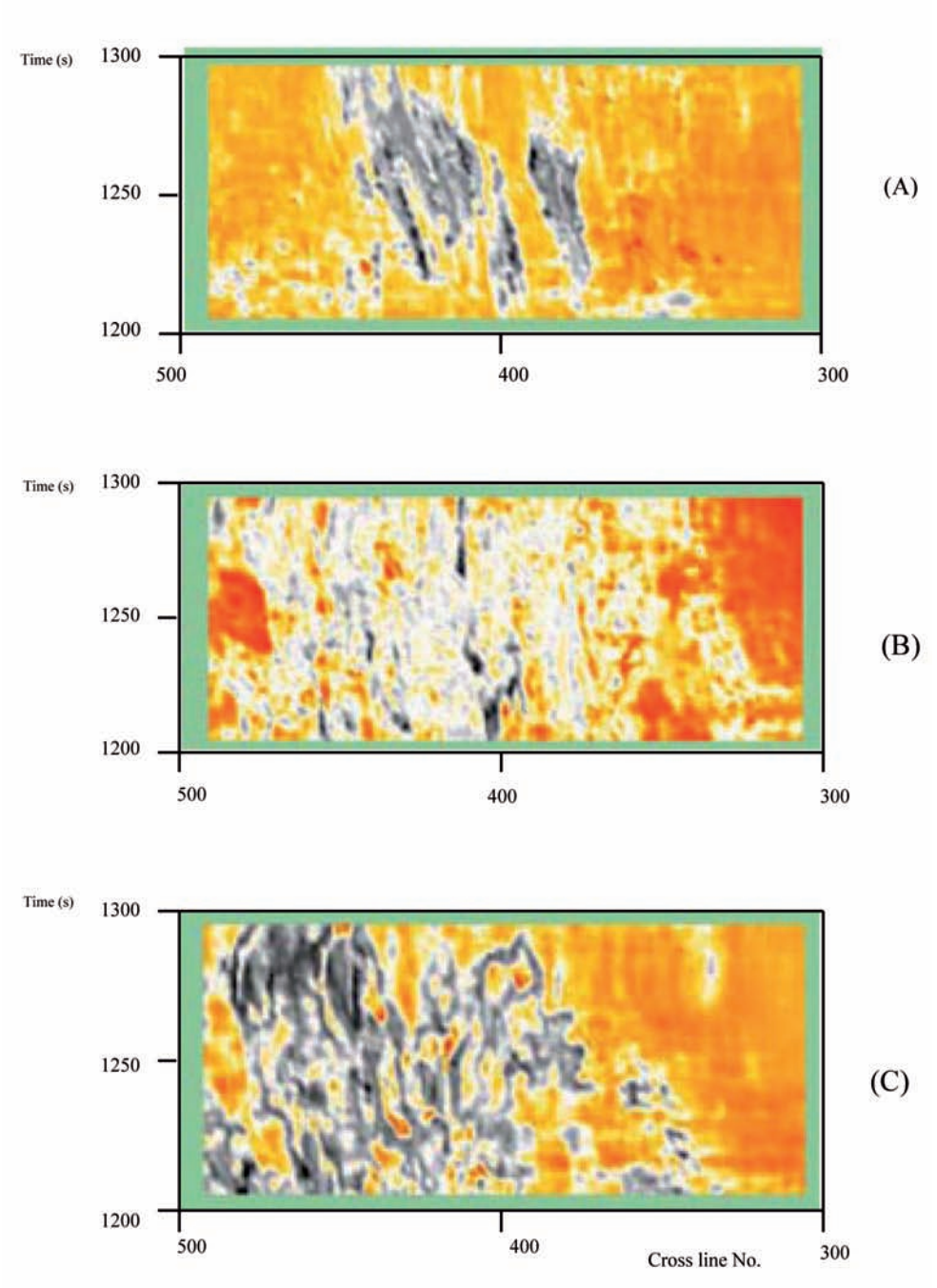

Fig. 12. Three different time slices above the fault cube. (A) 100 ms, (B) 200 ms and (C) 300 ms. The variation of fault orientation can be investigated by these time slices.

Fig. 13A shows inline 1250 on the fault cube where the faulted area is highlighted by gray and the non fault areas are in yellow.

To verify the superiority of the ANN procedure an attempt was made to compare the ANN fault prediction (Fig. 13A) with the fault prediction from conventional attributes like spectral decomposition (Fig. 13B) and coherency attribute (Fig. 13C). As it can be seen from this figure, the result obtained from the neural network (Fig. 13A) has better revealed the faulted areas than the other attributes in Figs. 13B and 13C.

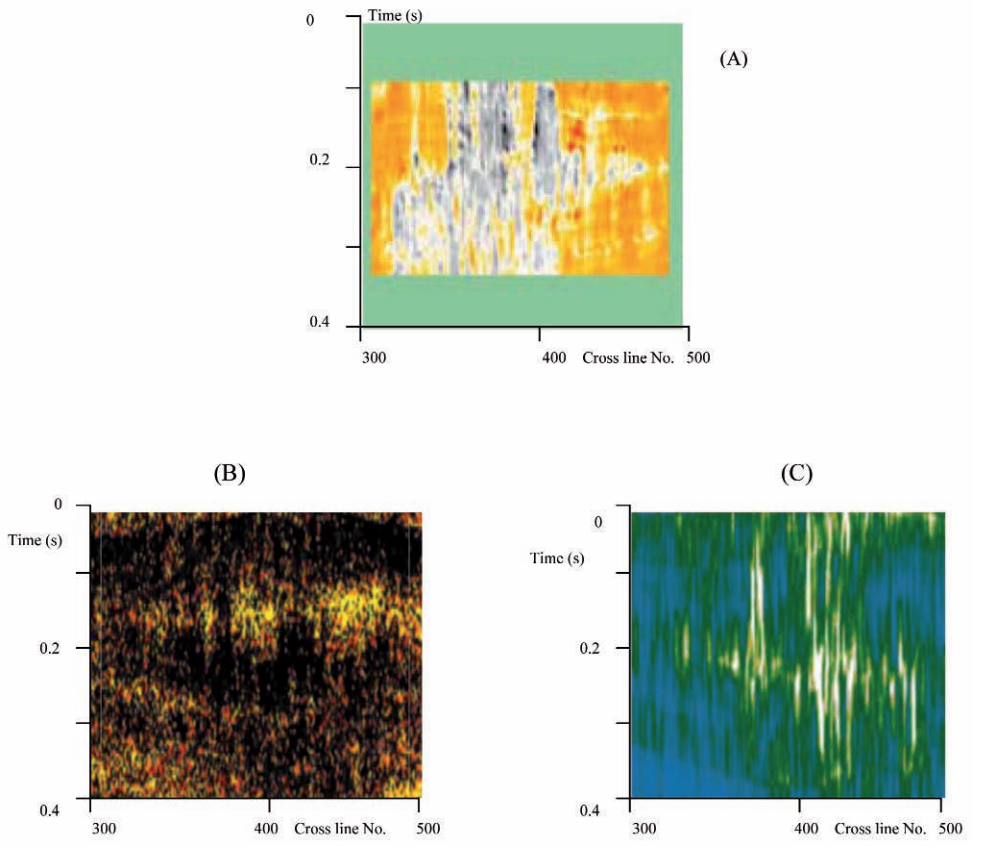

Fig. 13. (A) Inline 1250 on the fault cube. The faulted area is shown in gray and the non faulted areas are in yellow. (B) is the result from spectral decomposition for the same inline and (C) is the Coherency attribute result for the same inline. It can be seen that the fault cube (A) shows the fractured area clearer than the other attribute results.

Fig. 14 shows inline 1250 on the non fault cube. Here, the non faulted area is indicated by gray color and the faulted areas are in yellow. Comparison between inline 1250 and fault cube (Fig. 13A) shows that we can obviously detect the faulted areas clearly and with less uncertainty than the direct observation (Fig. 2).

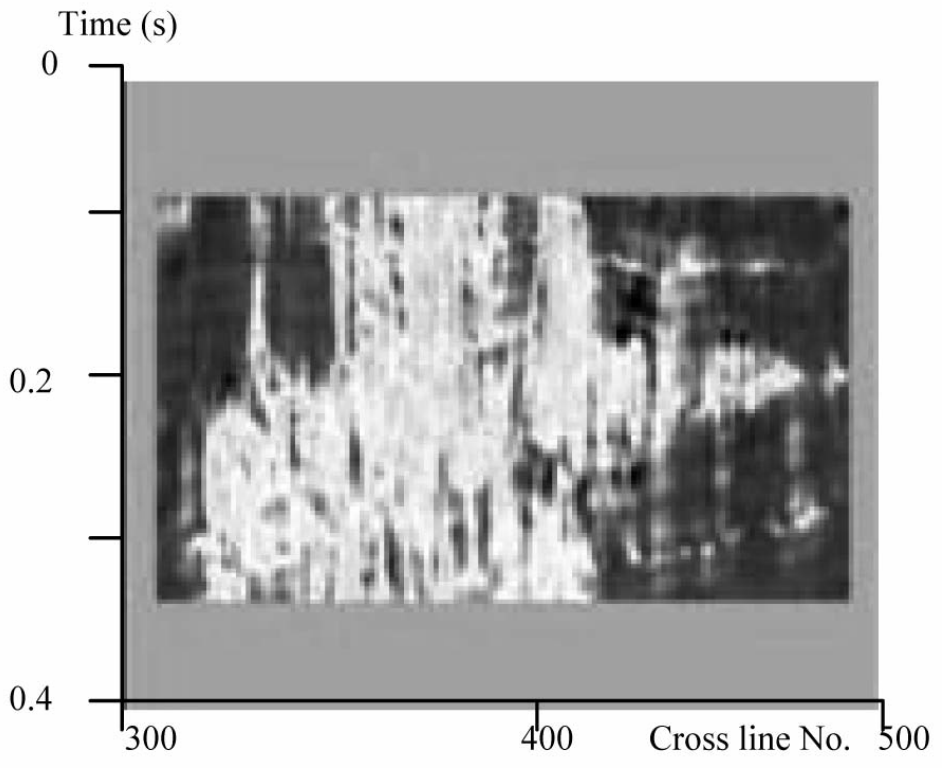

Fig. 14. Inline 1250 on the non fault cube, the non faulted area is indicated by gray and the faulted areas are in yellow.

CONCLUSION

There are several methods such as: single attribute study and direct manual fault picking for determining the location of minor faults. If the data quality is poor or a subtle fault is present on the seismic section, application of these approaches is inadequate. In order to overcome the related shortcomings, we have attempted to use the Artificial Neural Network (ANN) system as a transfer function. In this approach, the interpreter will select some places on the

seismic section that have high probability of being faults, the selected data are then input to the ANN system. When training of the system completes, the ANN system estimates an output cube that highlights the fault locations. In the single attribute study, application of a powerful attribute is necessary but in the ANN approach there is no limitation on the application of certain attributes for fault detection and the only condition that has to be taken into account is that different weights should be considered for different attributes in detecting fault location.

The integration of the seismic attribute method could define the location of minor faults in the cap rock more clearly than traditional methods of fault interpretation by manual picking or applying single attributes. This method is very useful for reservoir simulation and planning for oil production in other commercial seismic software.

ACKNOWLEDGMENTS

The authors greatly appreciate the support of the Institute of Geophysics and the Research Council of the Universities of Tehran and the University of Amirkabir which enabled them to provide this research. The authors are also grateful to Mr. Khorasani, for his unstinting help the respectable management of the Exploration Directorate of the National Iranian Oil Company (NIOC) who kindly provided the authors with collaboration and assistance in preparing real data for this study. We would like to acknowledge the dGB Software and Service and Professor Paul de Groot for providing us with an academic license of OpendTect for this research.

REFERENCES

Fomel, S., 2007. Local seismic attributes. Geophysics, 72: A29-A33.

Gao, D., 2003. Volume texture extraction for 3-D seismic visualization and interpretation. Geophysics, 68: 1294-1302.

Marfurt, K.J., Kirlin, R.L, Farmer, S.L. and Bahorich, M.S., 1998. 3-D seismic attributes using a semblance-based coherency algorithm. Geophysics, 63: 1150-1165.

Meldahl, P., Heggland, R., Bril, B. and de Groot, P., 1999, The chimney cube, an example of semi-automated detection of seismic objects by directive attributes and neural network. Part I: methodology. Expanded Abstr., 69th Ann. Internat. SEG Mtg., Houston: 931-931.

OpendTect manual software generated by DGB Company, Houston, Texas, U.S.A.

Roberts, A., 2001. Curvature attributes and their application to 3D interpreted horizons. First Break, 19: 85-100.

Tingdahl, K.M. and de Rooij, M., 2005. Semi-automatic detection of faults in 3-D seismic data. Geophys. Prosp., 53: 533-542.

West, B., May, S., Eastwood, J.E. and Rossen, C., 2002. Interactive seismic facies classification using textural and neural networks. The Leading Edge, 21: 1042-1049.